Hindawi Publishing Corporation
International Journal of Spectroscopy
Volume 2013, Article ID 485432, 8 pages
http://dx.doi.org/10.1155/2013/485432

Research Article

A Simulation Study of the Far-Infrared Absorption Spectra of HCl Diluted in Liquid Ar

A. Padilla and J. Pérez

Department of Fundamental and Experimental Physics, Electronics and Systems, University of La Laguna, Avenida Astrofísico Francisco Sánchez 38200, La Laguna, Spain

Correspondence should be addressed to A. Padilla; apadilla@ull.edu.es

Received 4 June 2013; Revised 31 July 2013; Accepted 15 August 2013

Academic Editor: Stefan Schmatz

The far-infrared absorption coefficient of HCl diluted in liquid Ar has been calculated by using a mixed classical-quantum stochastic simulation approach. The simulated spectra have been compared with the available experimental data at different thermodynamic conditions without using ad hoc fitting parameters. Despite the fact that some discrepancies can be observed in the high frequency side of the far-infrared bands, a reasonable agreement has been found between the theoretical and the experimental spectral profiles. Both, classical and quantum simulated line shapes were comparatively analyzed, determining the time scales involved in the rotational spectra.

1. Introduction

Infrared (IR) spectroscopy has been a useful tool in chemistry and physics to study and characterize a large variety of molecular systems. Because it is a nondestructive method, it is useful to study the structure of complex systems such as biological molecules, proteins, DNA, and membranes [1, 2]. In the last decade, IR spectroscopy has been used in the study of healthy and nonhealthy human tissues [2], and as well it has been employed in the industry field for quality control. On the other hand, IR spectroscopy has been highly successful in measuring the degree of polymerization in polymer manufacture [1, 2] and also has a forensic purpose, being used in the analyze of substances, such as alcohol, drugs, fibers, blood, and paints [2, 3].

Far-infrared spectroscopy is closely related to the rotational dynamics of a wide range of molecular systems. In particular, the study of far-infrared absorption spectra of diatomic polar molecules diluted in inert solvents gives relevant information about intermolecular interactions and the dynamical properties of the solvent variables involved in the diatomic relaxation [4, 5]. The rotational diatomic relaxation in dense fluids determines the basic properties of the far-infrared absorption bands, which, depending on the diatomic molecule and the thermodynamic conditions of the solution, can present a fine rotational structure associated with the R-branch of the gas phase spectra. In that case, as it happens with the HCl immerse in dense Ar [6], a quantum model for the diatomic rotation is necessary in order to explain the spectral properties of the far-infrared bands.

In a recent work [6], we have developed a mixed classical-quantum stochastic simulation (MCQSS) for the rotational and translational degrees of freedoms of both the solute HCl molecule and the Ar solvent atoms. In this study, the diatomic was treated as a quantum rotor which is coupled to the translational degrees of freedoms, both of the diatomic and the solvent atoms, which we use a classical stochastic approach for. By using this simulation technique, we studied the vibro-rotational fundamental bands of HCl diluted in dense Ar above and below the critical temperature. In this simulation, the effects of the solvent on the diatomic rotation were modelled by means of a directing intermolecular field (DIF), which is a variable associated with the dominant P_1 symmetry term of the solute-solvent anisotropic interaction. The DIF was considered as a stochastic noise of which characteristic parameters, the anisotropic interaction strength, and the binary autocorrelation time were calculated by means of molecular dynamics (MD) techniques using standard models for the intermolecular potentials.

In the present work, we have applied the MCQSS to the study of the far-infrared absorption bands of HCl diluted in liquid Ar over the liquid-vapour coexistence curve. Starting from the microscopic intermolecular potentials, we have calculated the pure rotational quantum bands of HCl in liquid Ar without using ad hoc fitting parameters. The simulated absorption coefficients were compared with the experimental far-infrared rotational bands, founding a reasonable agreement between them. On the other hand, the spectra calculated with the classical stochastic simulations (CSS, which are the classical limit of MCQSS) and MD simulations (which include effects discarded in CSS), adequately quantum corrected, were compared with both the experimental far-infrared profiles and the simulated MCQSS quantum spectra. Finally, the orientational relaxation times associated with the diatomic spectral density were determined, allowing a comparative analysis of the temporal scales involved in the far-infrared spectra.

The organization of the paper is as follows. A summary of the quantum stochastic approach together with the basis of the MD and CSS is described in Section 2. The comparison of the simulated and experimental spectra is presented in Section 3 along with a brief spectral analysis. Finally, some conclusions are shown in Section 4.

2. Techniques of Simulation

The basic model of our study considers a diatomic molecule immersed in an atomic solvent as a quantum rotor (small system S) coupled with the translational degrees of freedom of both the diatomic and the solvent (the bath B) by means of the anisotropic potential [6]

$$V_A\left(\vec{u},\left\{\vec{r}_p\right\}\right)=\sum_{q=-1}^{1}(-1)^q C_q^{(1)}(\vec{u})\,\lambda_{-q}\left(\left\{\vec{r}_p\right\}\right), \tag{1}$$

where $\vec{u}$ is the orientational unit vector of the diatomic, $\vec{r}_p$ is the vector joining the centre of mass of the diatomic to the pth solvent atom, $C_q^{(1)}(\vec{u})$ are the spherical components of the first rank modified harmonics $C^{(1)}(\vec{u})$ [7], and $\lambda_q(\{\vec{r}_p\})$ are the spherical components of the first rank DIF tensor $\lambda(\{\vec{r}_p\})$ given by

$$\lambda_q\left(\left\{\vec{r}_p\right\}\right)=\sum_p V^{(1)}\left(r_p\right)C_q^{(1)}\left(\vec{u}_p\right), \tag{2}$$

where $r_p = |\vec{r}_p|$, $\vec{u}_p = \vec{r}_p/r_p$ and the radial component $V^{(1)}(r_p)$ (see [6]) correspond to the functional form proposed by Holmgren et al. [8, 9].

The DIF $\lambda(t)$ is considered as a Gaussian stochastic process [6] where the basic parameters, the anisotropic interaction strength

$$\lambda^2=\langle\lambda(0)\cdot\lambda(0)\rangle \tag{3}$$

and the anisotropic correlation time

$$t_C=\int_0^\infty\left|\frac{\langle\lambda(t)\cdot\lambda(0)\rangle}{\lambda^2}\right|dt, \tag{4}$$

Table 1: Statistical parameters of the anisotropic interaction in reduced units ($\bar{\lambda}^2 = \lambda^2/hB_0c$) and ($\bar{t}_C = t_C 2\pi B_0 c$), where h is the Planck constant, c is the speed of light, and B_0 is the HCl rotational constant [10].

T (K)	108	115	120
ρ (g/cm^3)	1.25	1.20	1.15
$\bar{\lambda}^2$	53.3	53.3	52.9
$\bar{t}_C$	0.39	0.40	0.42
t_C (ps)	0.20	0.20	0.22

are determined by means of the MD, where $\langle\cdots\rangle$ denotes equilibrium average over the translation of diatomic and solvent atoms.

2.1. Molecular Dynamics Simulation. Classical MD relates the stochastic approach of the present model to the microscopic molecular structure of the HCl-Ar dissolution. The classical MD simulations were accomplished by considering a single HCl molecule and 250 argon atoms inside a cubic box, subject to periodic boundary conditions. The sizes of the boxes were chosen to fit in the experimental solvent density ρ at each thermodynamic state. The equations of motion were solved using a leapfrog Verlet algorithm, which includes a SHAKE technique to fix the diatomic bond length at $R_0 = 1.284$ Å and a coupling to the thermal bath in order to keep the system temperature T close to the solvent one. The time step was taken as $\Delta t = 2.5\times10^{-3}$ ps, and each simulation run involved a total of 10^6 time steps. Long enough equilibration periods were allowed before each simulation run.

The solvent densities used in the simulations were obtained along the liquid-vapour coexistence curve of Ar ($T < T_C = 151$ K) from the experimental solution temperatures using a cubic spline interpolation of the experimental data reported by Zelikina et al. [5]. Experimental temperatures and interpolated densities are shown in Table 1. Binary interactions between Ar atoms were modelled by the standard 6–12 Lennard-Jones potential ($\sigma = 3.405$ Å and $\epsilon = 119.8$ K) while the interaction for the HCl-Ar was approximated by a site-site potential adjusted to match the potential energy functions of Holmgren et al. [8, 9] (see [6]).

2.2. Mixed Classical-Quantum Stochastic Simulation (MCQSS). The spectral density of absorption for a spatial isotropic system is given by

$$I(\omega)=\frac{3}{\pi}\,\mathrm{Re}\left(\int_0^\infty\exp(i\omega t)\,C_{u_z}(t)\,dt\right) \tag{5}$$

while the absorption coefficient is proportional to

$$\alpha(\omega)\propto\omega\left(1-\exp\left(-\beta\hbar\omega\right)\right)I(\omega) \tag{6}$$

which will be normalized to unit maxima, where $\beta = 1/k_BT$, k_B is the Boltzmann constant, $\hbar$ is the Planck constant, and

$C_{u_z}(t)$ is the autocorrelation function associated with the z-component of $\vec{u}$, calculated under the noninitial correlation hypothesis as [6]

$$C_{u_z}(t) = \sum_{\eta=\pm1}\sum_{\eta'=\pm1}\sum_{jm}\sum_{j'm'}\sigma_j^0 \left\langle j'm' \left|u_z\right| j'+\eta'm'\right\rangle \times \left\langle j+\eta m \left|u_z\right| jm\right\rangle \left\langle C_{j'+\eta'm'}^{j+\eta m}(t)\, C_{j'm'}^{jm}(t)^*\right\rangle, \quad (7)$$

where σ_j^0 are the canonical populations of the diatomic rotor, $|jm\rangle$ are the usual eigenstates for the unperturbed rotor, $C_{j'm'}^{jm}(t)$ are the coefficients of the state $|jm(t)\rangle$ in the $|j'm'\rangle$ basis, and $\langle\cdots\rangle$ is the average over the translational degrees of freedom for both the solvent and the solute. The time evolution of the amplitudes $C_{j'm'}^{jm}(t)$ is given by

$$i\hbar\frac{d}{dt}C_{j'm'}^{jm}(t) = E_{j'}C_{j'm'}^{jm}(t) + \sum_{\eta=\pm1}\sum_{q=-1}^{1}(-1)^q \left\langle j'm'\left|C_q^{(1)}(\vec{u})\right| j'+\eta m'-q\right\rangle \times \lambda_{-q}(t)\, C_{j'+\eta m'-q}^{jm}(t), \quad (8)$$

where $E_{j'}$ are the free rotational energies, while the initial conditions are given by

$$C_{j'm'}^{jm}(0) = \delta_{jj'}\delta_{mm'}. \quad (9)$$

The numerical solutions of these equations define the quantum stochastic simulations of the spectral line shape (MCQSS). The system (8) was truncated at the value of $j_{\max} = 10$, while the rotational constant in the ground vibrational state was taken as the value averaged over the ^{35,37}Cl natural isotope abundances $B_0 = 10.436\,\text{cm}^{-1}$ [10]. The simulations were carried out by generating different time sequences of the DIF along a time interval of length $t = 2.4$ ps with time step of $\Delta t = 3.2\times10^{-3}$ ps, using the values of λ^2 and t_C obtained by means of MD (see Table 1). The average over the time sequences of the DIF was carried over a sample of 3×10^3 components [6].

2.3. Classical Stochastic Simulation. Classical stochastic simulations (CSSs) were carried out by solving the equations of motion for the orientational vector $\vec{u}$ and the angular velocity $\vec{\omega}$

$$\frac{d\vec{u}}{dt} = \vec{\omega}\times\vec{u}, \qquad I\frac{d\vec{\omega}}{dt} = \vec{u}\times\vec{\lambda}(t), \quad (10)$$

where $\vec{\lambda}(t)$ is the stochastic DIF and $I = \mu R_0^2$ is the moment of inertia of HCl being μ its reduced mass. In this case, different DIF sequences of length $t = 1.4$ ps and time step $\Delta t = 3.11\times10^{-3}$ ps were generated according to the values of λ^2 and t_C obtained with MD (see Table 1). The equations of motion (10) were solved using initial values of $\vec{\omega}(0)$, randomly chosen from the Maxwellian distribution and $\vec{u}(0)$ taken from a purely random uniform distribution of the orientation vector. The classical correlation function

$$C_u(t) = \langle\langle\vec{u}(t)\cdot\vec{u}(0)\rangle\rangle, \quad (11)$$

where the double bracket means average over both translation and rotation, was determined by using the noninitial correlation hypothesis and averaging over 3×10^4 sequences of DIF. The absorption spectral density

$$I(\omega) = \frac{1}{\pi}\int_0^\infty dt C_u(t)\cos(\omega t) \quad (12)$$

was corrected by introducing a semiclassical population factor [11]. The spectral density associated with the orientational correlation functions (11) determined by means of MD techniques was also corrected with the same procedure. For all types of orientational correlation functions, the orientational times are determined in the usual form [6]

$$\tau = 3\int_0^\infty \left|\text{Re}\left\{C_{u_z}(t)\right\}\right| dt = \int_0^\infty \left|\text{Re}\left\{C_u(t)\right\}\right| dt. \quad (13)$$

3. Spectral Study

In Figure 1, we have depicted the normalized (to unit maxima) experimental and theoretical MCQSS absorption coefficients of HCl diluted in liquid Ar at the coexistence liquid-vapour equilibrium states with temperatures $T = 108$ K, $T = 115$ K, and $T = 120$ K. The experimental details relative to the sample preparation, experimental conditions, HCl concentrations, and other experimental questions are given in [12]. In general terms, a reasonable agreement between the experimental and the theoretical absorption profiles can be observed. The main differences correspond to the fine rotational structure which is clearly more resolved in the MCQSS theoretical bands than in the experimental far-infrared profiles, where they are scarcely perceptible at the temperature $T = 120$ K and practically missing at lower temperatures. The same discrepancies were found when the theoretical MCQSS spectral densities were compared with the experimental vibro-rotational bands of HCl in dense Ar at subcritical and supercritical conditions [6]. The observed differences are probably due to the nature of the anisotropic potential of Holmgren et al. [8, 9], which, as it was commented by Hutson et al. [13], fails to reproduce the far-infrared and Raman pressure line broadening at low densities gas phase. As we will see, Holmgren potential produces a type of coherent hindered rotation which generates overestimated resolved rotational resonances.

We have also calculated the theoretical absorption coefficient of HCl in liquid Ar at the experimental states of this study (see Table 1), by using the anisotropic diatomic-solvent potential of Hutson et al. [13]. We have found that the rotational resonances are less resolved than for the Holmgren

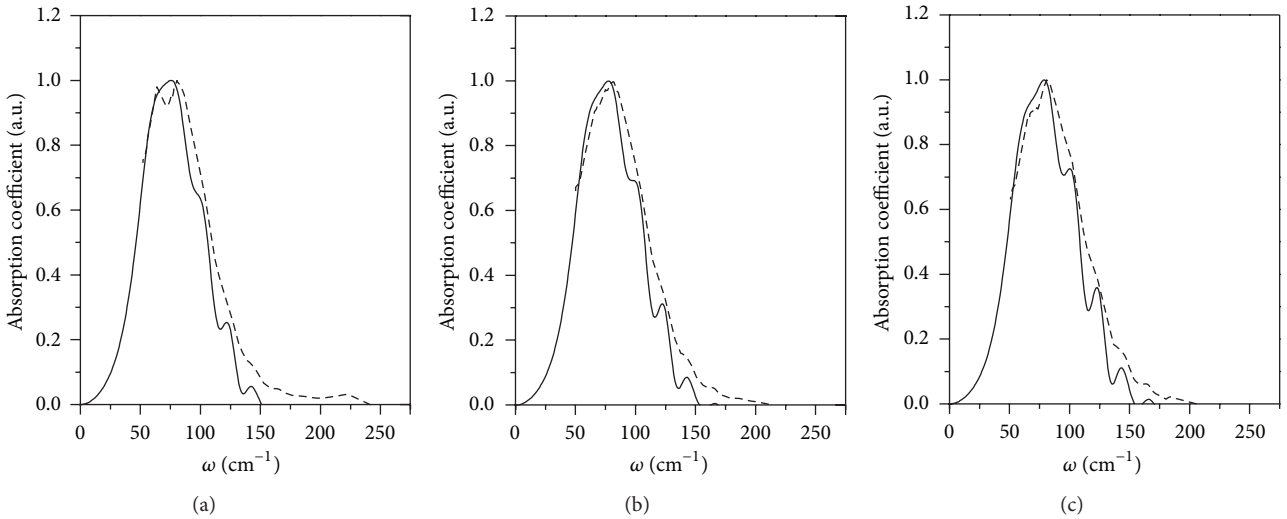

Figure 1: Experimental (dashed line) and MCQSS (continuous line) absorption coefficients (normalized to the maximum) of HCl diluted in Ar at the thermodynamic states: (a) $T = 108$ K, (b) $T = 115$ K, and (c) $T = 120$ K.

case [8, 9], but now, we have a worse overall theoretical-experimental agreement. On the other hand, Holmgren potential is able to explain the presence of the central Q-branch in the theoretical spectral densities, as it is observed in the experimental vibro-rotational spectral bands [6], while the Hutson spectral densities do not present the isolated diatomic forbidden Q-branch for the experimental thermodynamics states of this work and previous one [6]. Calculations carried out with other alternative potentials do not improve the results obtained with the Holmgren potential.

MCQSS absorption coefficients calculated in the current work have been determined without using any ad hoc fitting parameters. Unlike previous works [12, 14, 15], we have used the statistical parameters of the anisotropic interactions (3) and (4) (see Table 1) obtained by means of MD, employing realistic models for the HCl-Ar interaction. In earlier works, the statistical parameters were obtained by using microscopic cell models [15], by fitting theoretical and experimental spectra [14], or by using an erroneous estimation of the correlation times (4) [12]. Also, unlike previous theories, [12, 14, 15] based on the Kubo cumulant expansions, where it is not clear what specific statistical properties are assumed for the DIF tensor (2), in our work the kind of probabilistic properties assumed for the DIF is clear [6]. With this type of simulation, we solve the classical and quantum motion equations numerically without the need of truncating the cumulant expansions that lead to an unclear statistical hypothesis. On the other hand, MCQSS explain the presence of the Q-branch in the central part of the spectral density (5) [6], an effect largely unexplained with previous quantum spectral theories [14]. Perhaps the price to pay for all these improvements is a small discrepancy in the resolution of the rotational resonances.

The CSS absorption coefficients of HCl in liquid Ar at the thermodynamic states $T = 115$ K and $T = 120$ K are plotted in Figure 2 together with the experimental spectra. As in previous mixed classical-quantum cases, we can observe reasonable agreements between theoretical and experimental absorption bands, although in the high frequency side of the spectra, certain discrepancies can be noted. These are probably due to the difficulty of representing the high frequency region adequately by means of the classical dynamics. In fact, the high frequencies side of the absorption coefficient is the most affected by the quantum effects.

These same discrepancies are also observed in the MD calculations of the absorption coefficient, which are plotted in Figure 3 together with the CSS absorption coefficient at the thermodynamic states $T = 115$ K and $T = 120$ K. As it can be noted, the MD bands are very similar to the CSS line shapes, a fact also observed in the P- and R-branches of the rotational spectral density in the previous work [6] (we must note that spectral density is different from the absorption coefficient as in (5) and (6), having the rotational spectral density a triple P-Q-R branch structure for the Holmgren potential; see [6]). However, we note that in the previous paper [6], the Q-branch of the MD spectral density was stronger than in the CSS spectral density [6], also the same result has been obtained in the present study. The similitudes observed for the CSS and MD absorption coefficients indicate that, for this magnitude (6), the noninitial correlation hypothesis and the decoupling of the translation dynamics from the diatomic orientational motion are not very important, as opposed to the spectral density, where the Q branch at high densities is clearly different for MD and CSS profiles.

The agreement observed between the CSS and MD rotational bands with the experimental line shapes is mainly due to the scarcely presence of the rotational quantum structure in the experimental absorption coefficient of HCl in liquid Ar for the thermodynamic states considered. However, it is clear that quantum rotational effects are important in the HCl absorption coefficient, even for these thermodynamic conditions, mainly in the high frequency side of the higher temperatures states, where the experimental spectra show a very smooth structure of rotational resonances. This spectral region is dominated by the dynamics of the high rotational

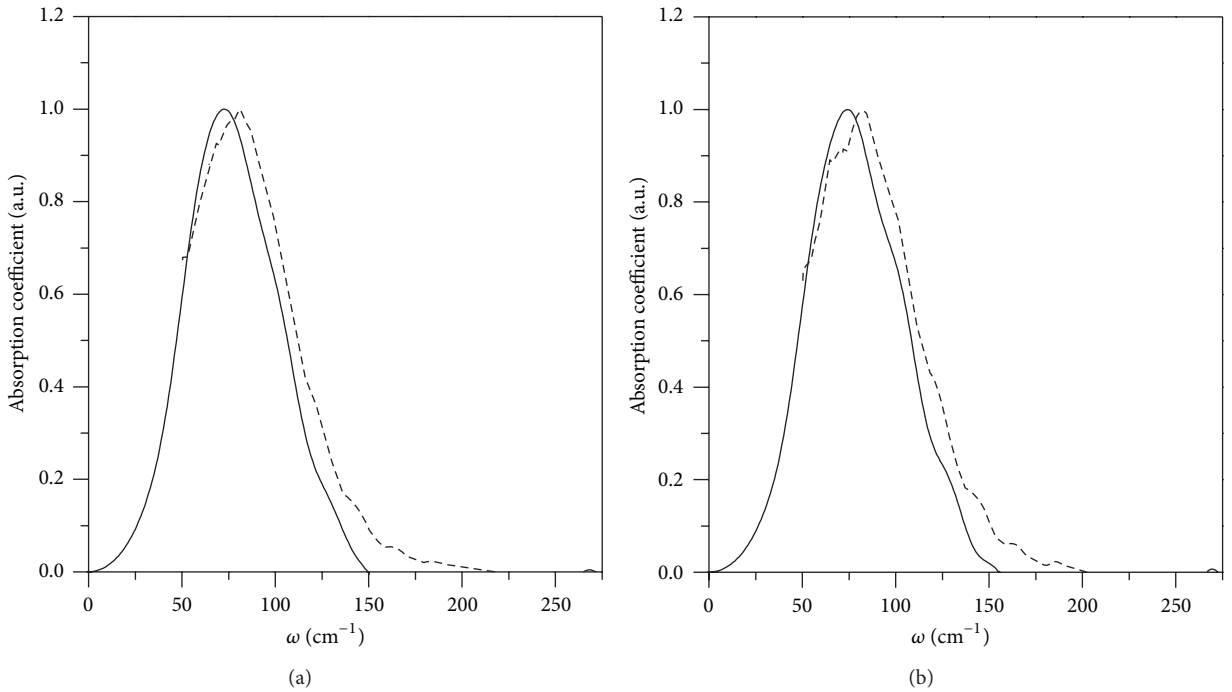

Figure 2: Experimental (dashed line) and CSS (continuous line) absorption coefficients (normalized to the maximum) of HCl diluted in Ar at the thermodynamic states: (a) $T = 115$ K and (b) $T = 120$ K.

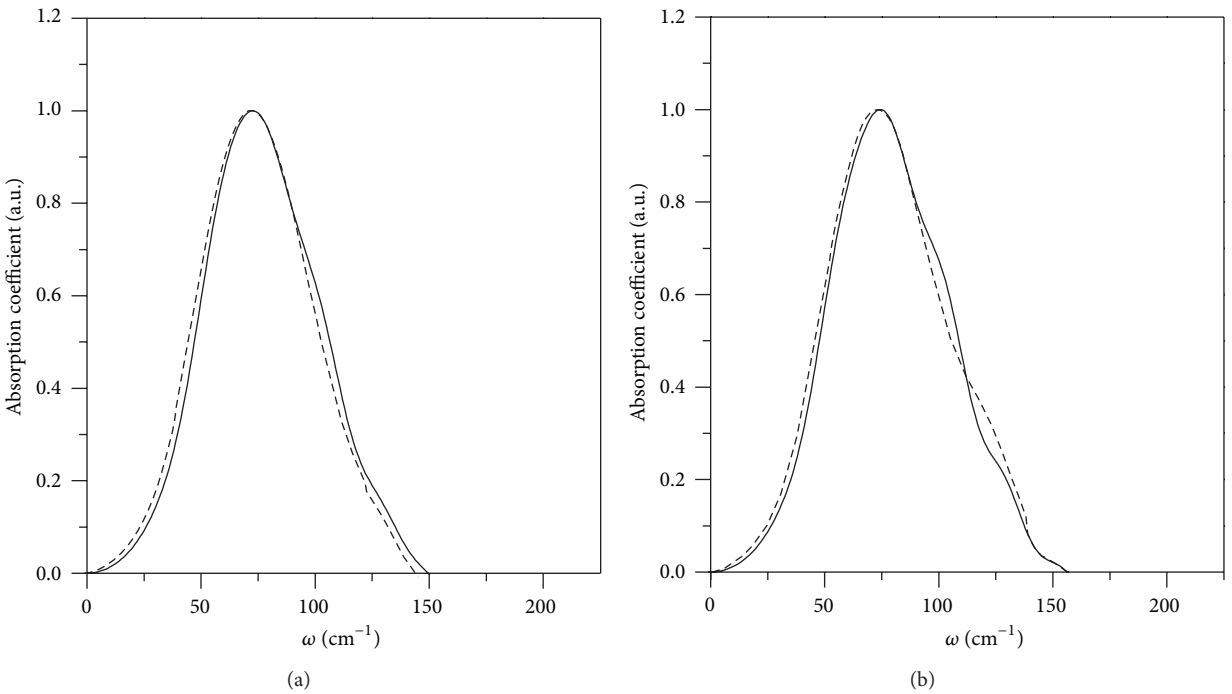

Figure 3: MD (dashed line) and CSS (continuous line) absorption coefficients (normalized to the maximum) of HCl diluted in Ar at the thermodynamic states: (a) $T = 115$ K and (b) $T = 120$ K.

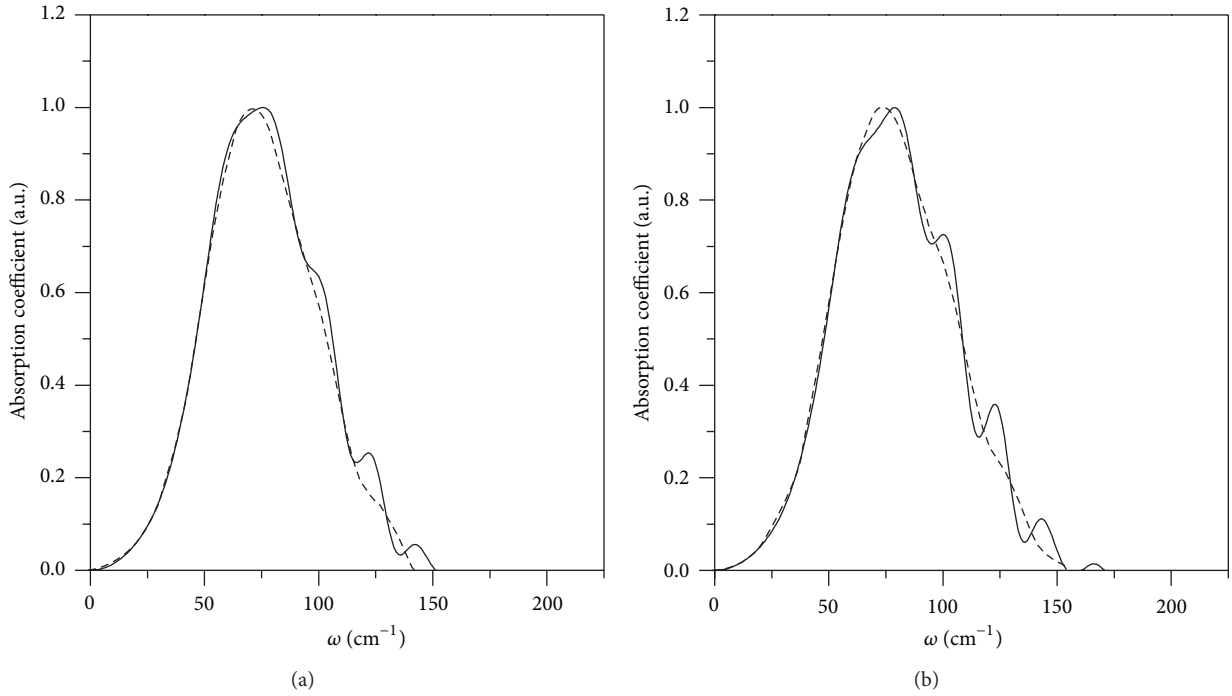

Figure 4: MCQSS (continuous line) and CSS (dashed line) absorption coefficients (normalized to the maximum) of HCl diluted in Ar at the thermodynamic states: (a) $T = 108$ K and (b) $T = 120$ K.

states which are appreciably populated for the experimental temperatures of this work (see Table 1) ($j = 6$–10). These states have been traditionally modelled by means of quasifree rotation approach and successfully represented by the modified rotor model of Pérez et al. [14], although they require the use of fitting parameters.

In Figure 4, we have plotted the MCQSS absorption coefficient and the CSS pure rotational bands at the thermodynamic states $T = 108$ K and $T = 120$ K. We can observe again that both types of spectra show a clear similitude between them. In this case, both MCQSS and CSS absorption coefficients coincide in the low frequency range, while in the high frequency region, this coincidence is limited to the similitude between the envelope of the MCQSS rotational structure and the CSS spectral profile. A similar result was obtained in a previous work [6] where the classical and mixed classical-quantum P- and R-branches of HCl in Ar were compared.

The correlation time t_C is a key element in the rotational dynamic of HCl diluted in liquid Ar. By using MD techniques, we have obtained values of the anisotropic correlation times t_C associated with the DIF in the thermodynamic states analyzed in this study (see Table 1). The obtained values are greater than those previously determined by fitting procedures [14] or with microscopic cell models [15]. Similar results were obtained in a previous work [6]. The magnitude of these correlation times is closely related to the apparition of the central Q-branch in the spectral density and also with the resolution of the rotational resonances in the quantum simulated absorption coefficient. By reducing t_C at constant λ^2 it can be observed how the rotational resonances are broadened and the Q-branch disappears. Further, with the values of the statistical parameters λ^2, and t_C shown in Table 1, the traditional spectral theories based in Kubo's cumulant expansions [14, 15] predict absorption coefficients with a rotational structure extremely resolved. This extreme resolution is basically due to the magnitude of the anisotropic correlation times t_C which, as it happens in the previous work [3], are greater than the orientational correlation times (13) associated with the orientational correlation functions (see, (7) and (11)).

Table 2: Orientational correlation times associated with the MCQSS, CSS, and MD absorption coefficients of the HCl diluted in liquid Ar.

T (K)	108	115	120
τ_{MCQSS} (ps)	0.160	0.158	0.158
τ_{CSS} (ps)	0.157	0.154	0.152
τ_{MD} (ps)	0.147	0.149	0.136

In Table 2, we have shown the values of the orientational times τ of HCl in Ar, corresponding to MCQSS, CSS, and MD spectral densities at the different thermodynamic states of this study. As it can be observed, the orientational correlation times are in the subpicosecond time scale, and as in the present work, the temperature range is not wide, and the values of the orientational correlation times do not change too much in the different thermodynamic states.

In general terms, a weak decreasing of τ with increasing temperature is observed, and as in [6], the quantum correlation times are slightly greater than the classic ones. It can be seen that in all cases (see Tables 1 and 2), the anisotropic correlation times are clearly greater than the orientational correlation ones. This means that the diatomic orientational relaxation takes place outside the Markovian limit, being hindered by an anisotropic potential which presents a certain temporal coherence, producing effects like the apparition in the central part of the spectral density between the P- and R-branches, the so called Q-branch [6], which in the high density states of this study is associated with the long-lived diatomic-solvent spatial correlations and in the low density limit, it leads to the traditional Van der Waals complexes [16].

The influence of the Q-branch (present in the spectral density (5); see [6]) over the far-infrared absorption profile (6) is small, but we have referred to this type of branch because it is a spectral effect that during a long time has failed to have a clear explanation, and the simulations developed in this work and in previous ones [6] have been reasonably reproduced in a quantum system. An extensive classical study of the Q-branch has been accomplished by Medina et al. [17–20].

Finally, the presence of a fine rotational structure and the apparition of Q-branch were traditionally understood as effects due to two different origins. In the current work, in contrast to previous theories [14, 15], it has been shown there is not a separation between nearly-free rotation and hindered rotation, with the first being responsible for the resolved rotational structure (more clearly observed in absorption coefficient) and the second being responsible for the central Q-branch (observed in the spectral density). Now, we have a coherent (large t_C) hindered rotation that produces both resolved rotational resonances and the central Q-branch.

4. Summary and Conclusions

We have made a mixed classical-quantum stochastic simulation study of the far-infrared spectra of HCl diluted in liquid Ar. This approach had been used in a previous work [6] where the fundamental bands of HCl in dense Ar below and above the critical temperature were studied. Both mixed classical-quantum and pure classical simulations were made in one case stochastic and in other case of MD type. In the stochastic case, the basic statistical parameters used in the simulations were determined by means of MD using definite models of the atomic binary potentials. In all cases, the simulated spectra did not require any ad hoc fitting parameter.

The MCQSS reproduces the basic features of the experimental far-infrared absorption coefficient of the HCl diluted in liquid Ar, although the theoretical bands present a rotational structure clearly more resolved than the experimental discrete resonances, which is scarcely perceptible in the less dense thermodynamic states. These discrepancies are probably due to the nature of the HCl-Ar binary potential of Holmgren et al. [8, 9], that, as it is known, does not reproduce the far-infrared and Raman pressure broadening at low gas densities [13], producing a kind of coherent hindered rotation which overestimates the narrowing of the rotational resonances and reproduces satisfactorily the isolated diatomic forbidden Q branch (in the spectral density).

Since the experimental spectra do not have a clearly resolved quantum rotational structure, both the CSS and the MD absorption coefficients of HCl in Ar reproduce the basic aspect of the experimental line shape. We have found similitudes between the CSS and MD far-infrared absorption bands and also between the MCQSS and the CSS spectra. The first one indicates that the approach assumed in the stochastic simulations for the absorption coefficient is reasonable for the thermodynamics conditions of this study, and the second one indicates that quantum effects are not dominant in this study.

We have obtained that the anisotropic correlation times t_C (4) are greater than the orientational correlation ones (see Tables 1 and 2), taking place the orientational relaxation outside the Markovian limit, a fact which produces effects such as the apparition in the spectral density of the central Q branch [6], and the overestimated narrowing of the rotational resonances. Both effects are caused by the same mechanism, the coherent hindering of the diatomic reorientation.

Finally, in this work, we have checked that both the near-infrared spectra of HCl in dense Ar [6] and the far-infrared spectra of HCl diluted in liquid Ar can be reasonably reproduced by the mixed classical-quantum stochastic model developed in [6] and that this analysis will be useful in order to describe the diatomic environment by means of a more completed dynamical model.

Acknowledgments

The authors would like to thank M. O. Bulanin for the many helpful discussions in the scope of this line of research and Pedro N. Leal for his carefully reading of the paper. The authors also acknowledge financial support from the Canary Islands Regional Government (Consejería de Educación, Cultura y Deportes del Gobierno de Canarias) under the Project 2008/00000233.

References

[1] T. Theophanides, Ed., *Infrared Spectroscopy—Material Science, Engineering and Technology*, InTech, Vienna, Austria, 2012.

[2] T. Theophanides, Ed., *Infrared Spectroscopy—Life and Biomedical Sciences*, InTech, Vienna, Austria, 2012.

[3] J. Uddin, Ed., *Macro to Nano Spectroscopy*, InTech, Vienna, Austria, 2012.

[4] J. R. Birch and J. Yarwood, *Spectroscopy and Relaxation of Molecular Liquids*, D. Steele and J. Yarwood, Eds., Elsevier, Amsterdam, The Netherlands, 1991.

[5] M. O. Bulanin, N. D. Orlova, and G. Ya Zelikina, *Molecular Cryospectroscopy. Advances in Spectroscopy*, R. J. Clark and R. E. Hester, Eds., Wiley, Chichester, UK, 1995.

[6] A. Padilla, J. Pérez, W. A. Herrebout, B. J. Van der Veken, and M. O. Bulanin, "A simulation study of the vibration-rotational spectra of HCl diluted in Ar: rotational dynamics and the origin of the Q-branch," *Journal of Molecular Structure*, vol. 976, no. 1–3, pp. 42–48, 2010.

[7] R. Zare, *Angular Momentum*, Wiley, New York, NY, USA, 1988.

[8] S. L. Holmgren, M. Waldman, and W. Klemperer, "Internal dynamics of van der Waals complexes. I. Born-Oppenheimer separation of radial and angular motion," *Journal of Chemical Physics*, vol. 67, no. 10, Article ID 4414, 9 pages, 1977.

[9] S. L. Holmgren, M. Waldman, and W. Klemperer, "Internal dynamics of van der Waals complexes. II. Determination of a potential energy surface for ArHCl," *Journal of Chemical Physics*, vol. 69, no. 4, Article ID 1661, 9 pages, 1978.

[10] G. Guelachvili, P. Niay, and P. Bernage, "Infrared bands of HCl and DCl by Fourier transform spectroscopy. Dunham coefficients for HCl, DCl, and TCl," *Journal of Molecular Spectroscopy*, vol. 85, no. 2, pp. 271–281, 1981.

[11] P. H. Berens and K. R. Wilson, "Molecular dynamics and spectra. I. Diatomic rotation and vibration," *Journal of Chemical Physics*, vol. 74, no. 9, Article ID 4872, 11 pages, 1981.

[12] W. A. Herrebout, B. J. Van Der Veken, A. Medina, A. Calvo Hernández, and M. O. Bulanin, "Experimental and theoretical study of the far-infrared spectra of HCl dissolved in liquid Ar, Kr, and Xe," *Molecular Physics*, vol. 96, no. 7, pp. 1115–1124, 1999.

[13] J. M. Hutson, "Vibrational dependence of the anisotropic intermolecular potential of Ar-HCl," *The Journal of Physical Chemistry*, vol. 96, no. 11, pp. 4237–4247, 1992.

[14] M. O. Bulanin, K. Kerr, A. Padilla, J. Pérez, and A. C. Hernández, "First vibrational overtone bandshape of HCl in fluid SF_6: an experimental and theoretical study," *Physical Chemistry Chemical Physics*, vol. 2, no. 23, pp. 5375–5382, 2000.

[15] L. Bonamy and P. N. M. Hoang, "Far infrared absorption of diatomic polar molecules in simple liquids and statistical properties of the interactions. I. Spectral theory," *The Journal of Chemical Physics*, vol. 67, pp. 4423–4430, 1977.

[16] K. G. Tokhadze and Z. Mielke, "About origin of Q component on the vibration-rotation band of HF in simple solvents," *The Journal of Chemical Physics*, vol. 99, no. 7, pp. 5071–5077, 1993.

[17] A. Medina, J. M. M. Roco, A. C. Hernández et al., "Vibration-rotation spectra of HCI in rare-gas liquid mixtures: molecular dynamics simulations of Q-branch absorption," *Journal of Chemical Physics*, vol. 116, no. 12, pp. 5058–5065, 2002.

[18] A. Medina, J. M. M. Roco, A. C. Hernández, and S. Velasco, "Infrared Q-branch absorption and rotationally-hindered species in liquids," *Journal of Chemical Physics*, vol. 119, no. 10, pp. 5176–5184, 2003.

[19] A. Medina, J. M. M. Roco, A. C. Hernández, and S. Velasco, "Infrared spectral profiles in liquids and atom-diatom interactions," *Journal of Chemical Physics*, vol. 121, no. 13, pp. 6353–6360, 2004.

[20] A. Medina, J. M. M. Roco, A. C. Hernández, and S. Velasco, "Dynamical characterization of rotationally hindered species in liquids," *Journal of Chemical Physics*, vol. 123, no. 23, Article ID 234509, 7 pages, 2005.